

See discussions, stats, and author profiles for this publication at: <https://www.researchgate.net/publication/338061167>

# Hydrothermal-Assisted Transient Binder Jetting of Ceramics for Achieving High Green Density

Article in JOM: the journal of the Minerals, Metals & Materials Society · December 2019

DOI: 10.1007/s11837-019-03962-2

CITATIONS

2

READS

1,065

5 authors, including:



Fan Fei

University of Iowa

11 PUBLICATIONS 31 CITATIONS

[SEE PROFILE](#)



Baizhuang Zhou

University of Iowa

1 PUBLICATION 2 CITATIONS

[SEE PROFILE](#)



Xuan Song

University of Iowa

42 PUBLICATIONS 1,328 CITATIONS

[SEE PROFILE](#)

Some of the authors of this publication are also working on these related projects:



Biomimetic structures, 3D printing, carbon nanotube, electrical alignment [View project](#)



# Hydrothermal-Assisted Transient Binder Jetting of Ceramics for Achieving High Green Density

FAN FEI,<sup>1</sup> LI HE,<sup>1</sup> BAIZHUANG ZHOU,<sup>1</sup> ZIYANG XU,<sup>2</sup>  
and XUAN SONG<sup>1,3</sup> 

1.—Department of Industrial and Systems Engineering, The Iowa Technology Institute, The University of Iowa, Iowa City, IA 52242, USA. 2.—Department of Mechanical Engineering, The University of Iowa, Iowa City, IA 52242, USA. 3.—e-mail: xuan-song@uiowa.edu

Ceramic additive manufacturing (AM) provides a freeform fabrication method for creating complex ceramic structures that have been extremely difficult to build by traditional manufacturing processes. However, ceramic structures made by AM processes usually exhibit a relatively low density, which is largely due to the use of a large amount of organic binder in shaping green bodies. In this research, we present a new ceramic AM process, named hydrothermal-assisted transient binder jetting (HTBJ), which utilizes a water-based hydrothermal mechanism to fuse particles, eliminating the use of binders in forming green bodies. A prototype system for the proposed HTBJ process is introduced. The effects of process parameters (such as layer thickness, printing passes, prepressing and final pressing pressure, and temperature) on the properties of achieved green parts are investigated. Experimental results indicate that, with optimized process parameters, HTBJ can achieve three-dimensional ceramic green parts with a high density of up to 90%.

## INTRODUCTION

Additive manufacturing (AM) provides a freeform fabrication method for creating complex ceramic structures that have been extremely difficult to build by traditional manufacturing processes. Several AM processes have been successfully applied in the fabrication of complex ceramic structures, such as stereolithography (SL),<sup>1–3</sup> selective laser sintering,<sup>4–6</sup> binder jetting (BJ),<sup>7–9</sup> etc. However, ceramic structures made by AM processes usually exhibit a much lower density than their traditionally manufactured counterparts, which is largely due to the need for high volume fractions of organic binders for shaping green parts in ceramic AM processes. In SL processes, for example, a volume fraction up to 70 vol.% of a photopolymer resin is used to bind the ceramic particles together, which results in a low green part density and, consequently, a low final density after the sintering processes.

Numerous research efforts have been made to enhance the ceramic densities achieved by AM processes. A straightforward method is to enhance particle packing density via optimizing process parameters, such as layer thickness and particle

size distribution.<sup>9,10</sup> Another route is through post-processing ceramic green bodies or final parts, such as cold compaction,<sup>11</sup> porosity infiltration,<sup>12–16</sup> hot isostatic pressing (HIP),<sup>17–19</sup> etc. Emerging approaches have been focused on developing nanoparticle-suspension-based binders, which increase the density through occupying interparticle pores with the suspended nanoparticles.<sup>20–23</sup> All these methods can mitigate a limited amount of interparticle pores in the final ceramic parts, but are still restricted in achieving high-density ceramics, in particular, monolithic ceramics.

In nature, rocks are formed from particle sediments through a natural lithification process, which does not use any organic binders to bind particles. As shown in Fig. 1, the lithification of particle sediments into a natural rock involves two basic steps: compaction and cementation. Compaction is the rearrangement of particle sediments due to the intense pressing weight of overlying sediments. Cementation is a process whereby groundwater carries dissolved minerals into the empty spaces between the loose particle sediments and crystallizes new minerals between the sediment grains. Under relatively mild temperatures and pressure, these

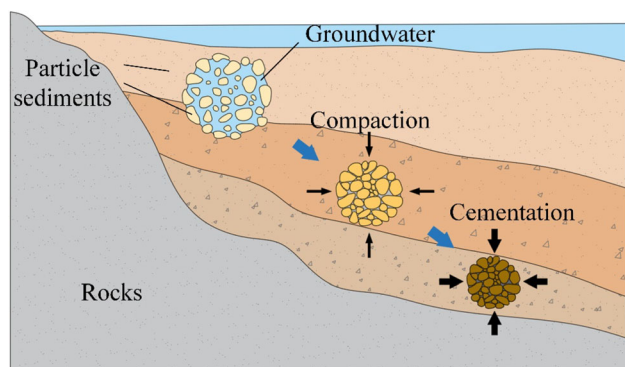


Fig. 1. Lithification process of rock in nature.

processes only require groundwater to bind particles, providing a potential route for obviating the need for a large amount of organic binders in ceramic AM. We obtained inspiration from the lithification process and developed a new AM method for ceramics, named hydrothermal-assisted transient binder jetting (HTBJ). The HTBJ processes selectively fuse particles by simply depositing a transient solution, such as water, into a powder bed, followed by exposing the powder to a controlled hydrothermal environment. The process can potentially achieve high-density ceramics parts without introducing any secondary phase.

## METHODS

### Materials

In this research, vanadium oxide ( $V_2O_5$ , 98%; Sigma-Aldrich, St. Louis, USA) was selected as a model material, and is an inorganic compound widely used as industrial catalysts and as thermally-resistant materials.<sup>24</sup> The particle size of the material is  $1\ \mu\text{m}$ , and the melting point is  $690^\circ\text{C}$ . The powder exhibits a partial solubility in water, which enables the selective consolidation of the material in the proposed HTBJ process (more discussion in “Results and Discussion” section). To improve the powder flowability for coating layers with smaller thicknesses, the raw  $V_2O_5$  powders were first mixed with an ethanol solution and washed in an ultrasound bath. The mixed powders were then dried and ground into fine powders using a mortar and pestle. This powder preparation method reduced the agglomerates in the raw  $V_2O_5$  powder and allowed for the coating of the particle layers with a small layer thickness, e.g.,  $100\ \mu\text{m}$ , in contrast to the  $500\ \mu\text{m}$  achieved with the raw powder.

Distilled (DI) water and a commercial aqueous ink (PG-243; Canon) were used as transient solutions, which fused the ceramic nanoparticles through a mediated dissolution–diffusion–precipitation process under the transient evaporation of the solvent. The aqueous ink is composed of 60–80% water, 5–10% Glycerin, 5–10% Lactam, and 5–10% Glycol.

### Fabrication Process

The proposed HTBJ process involves three major steps to achieve a green part with high density: transient solution deposition, hydrothermal pressing, and ultrasonic elimination, as shown in Fig. 2. An inkjet 3D printer was used to selectively deposit a transient aqueous solution into a ceramic powder bed in a target 3D shape. The ceramic nanoparticles in the powder bed, including the transient-solution-wetted nanoparticles and dry nanoparticles, were then compacted under a controlled hydrothermal environment applied via a uniaxial press. A 3D object with the target shape (i.e., green part) was obtained after ultrasonic cleaning. Finally, the green part can be fully densified through post-consolidation processes, such as furnace sintering. The three steps used to create green parts are discussed in detail in the following sections.

### Inkjet-Printing-Based Transient Solution Deposition

An inkjet 3D printer was developed to selectively deposit a transient solution in a ceramic powder bed; a prototype system is shown in Fig. 3. The system was composed of a building platform, a powder reservoir, a powder feeding roller, and an inkjet printhead, dissected from a Canon inkjet printer. A belt-pulley mechanism was used to move the inkjet printhead and the roller along the  $x$  axis. The building platform and the powder reservoir were controlled independently by a  $z$ -axis linear actuator. On initialization of the fabrication, the following steps occurred: (1) the building platform moved down a distance of  $d$  ( $d$  is the layer thickness, e.g.,  $200\ \mu\text{m}$ ); (2) the powder reservoir moved up a certain distance to feed ceramic nanoparticles into the working area; (3) the roller rotated counter-clockwise and moved from left to right to spread a thin layer of ceramic nanoparticles on top of the building platform; the packing density of the fresh layer can be further increased by manual or hydraulic pressing; and (4) as the inkjet printhead moved together with the roller, it deposited a transient solution with a predefined 2D pattern into the new layer. The amount of the deposited transient solution was controlled by repeating step (4) with different numbers of printing passes. These steps were repeated until the whole part was completed.

### Analysis of Process Parameters

Key process parameters associated with the HTBJ process are given in Table I.

Process parameters, including layer thickness, print pass, pre-press pressure, ink viscosity and surface tension, influence the penetration and diffusion of a deposited transient solution in the powder bed, which consequently affect the concentration of a transient solution in the powder bed.

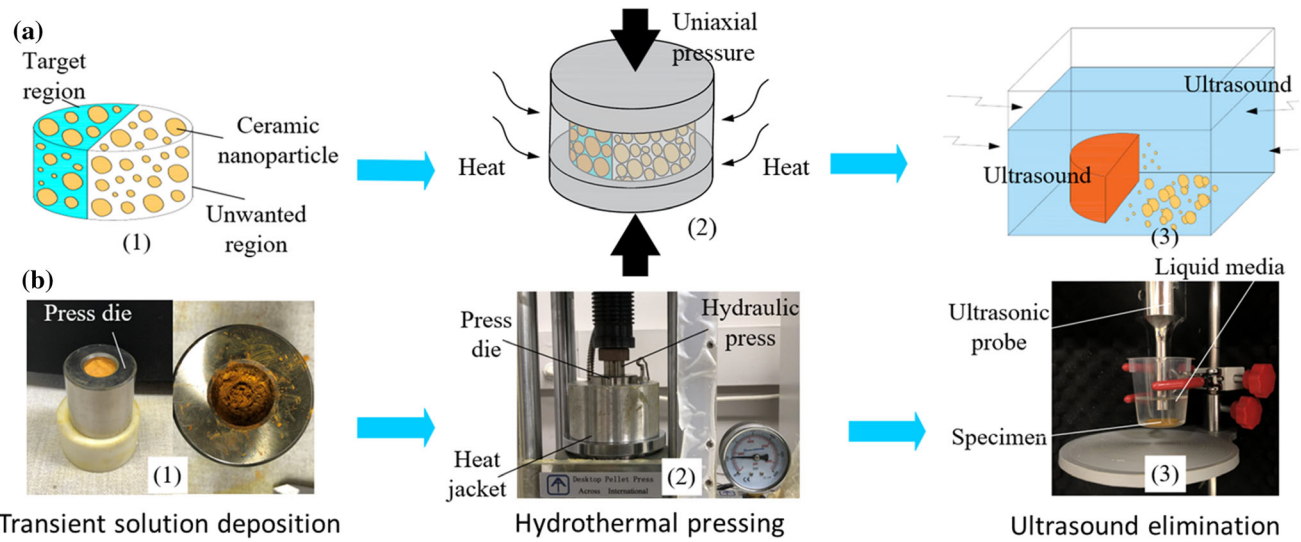


Fig. 2. The HTBJ process: (a) schematic illustration; (b) experimental setups.

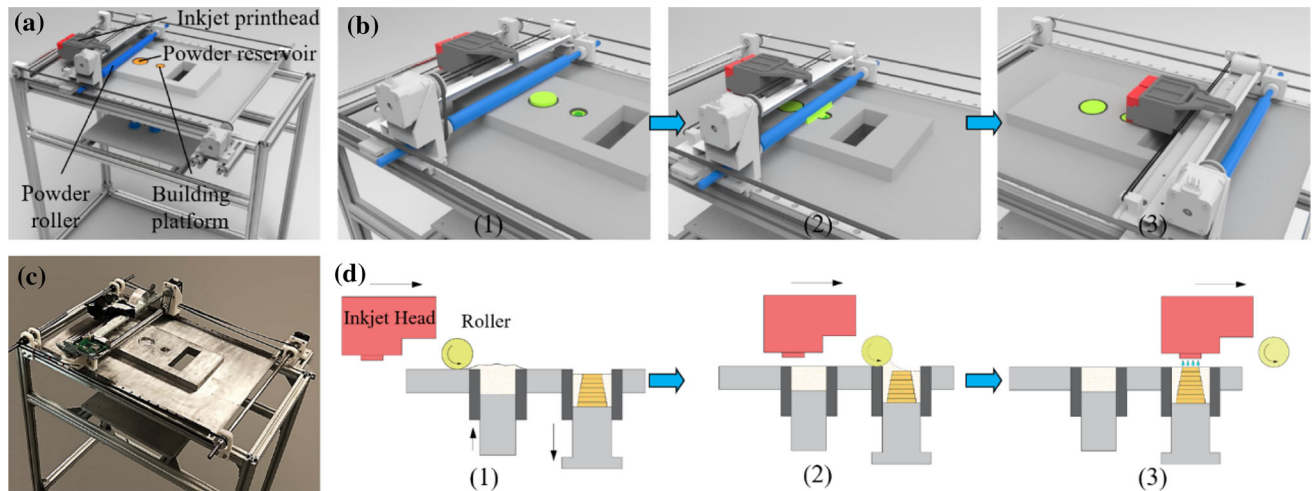


Fig. 3. Transient solution deposition via inkjet printing: (a) design of an inkjet 3D printer; (b) 3D schematic of transient solution deposition; (c) a prototype system of the inkjet 3D printer; (d) 2D schematic of transient solution deposition.

Table I. Process parameters in the HTBJ process

Process parameter	Explanation
Layer thickness	The thickness of each layer
Print pass	The printing times of the same layer in each layer
Pre-press pressure	The pressure applied to each new layer after powder coating
Final pressure	The pressure applied to the powder compact during hydrothermal pressing
Temperature	The temperature applied to the powder compact during hydrothermal pressing
Ink viscosity	The viscosity of the transient solution containing water and surfactant
Ink surface tension	The surface tension of the transient solution

The concentration of a transient solution, on the other hand, determines the temperature and pressure required for achieving differential consolidation of the wetted and dry nanoparticles. To understand the effects of process parameters on

the consolidation of nanoparticles, several sample disks were made by manually mixing  $V_2O_5$  powders with DI water at different concentrations (0–30 wt.%). The mixed powders were hydrothermally pressed under different final pressures



(250,650 MPa) and temperatures (120°C and 140°C). Scanning electron microscopy (SEM) was used to study the microstructures of samples built by different process parameters. The green density of the samples was measured using ASTM C373-88.

### Construction of Processing Map

As mentioned above, the temperature and final pressure used in hydrothermal pressing are dependent on the concentration of a transient solution deposited in the powder compact, all of which influence the achieved green density and strength. We constructed a processing map for selecting the proper temperature and final pressure that can fully fuse the wetted nanoparticles without influencing the dry nanoparticles. We used DI water as the transient solution and mixed the powder with water at a constant water concentration, i.e., 10 wt.%. The mixed powder was hydrothermally pressed under pressures ranging from 12.5 MPa to 50 MPa and temperatures from 25°C to 200°C. The achieved ceramic compacts were smashed in ethanol in an ultrasound cleaner for 15 min before the morphology of the compacts was evaluated (e.g., full disk, partially smashed, or completely smashed).

## RESULTS AND DISCUSSION

### Fusion Mechanisms in HTBJ

In the proposed HTBJ process, ceramic nanoparticles in the powder bed were selectively fused by controlling the deposition of a water-based transient solution. Under a proper hydrothermal environment, nanoparticles wetted by the transient solution can be fused, while the dry nanoparticles remained loose. The exact mechanisms governing this water-modulated consolidation of ceramic nanoparticles are very complicated and have not yet been well understood, but an important component involved can be attributed to the hydrothermal interaction between the transient solution and the

nanoparticles, which mediates a dissolution–diffusion–precipitation process of mass at nanoparticle surfaces,<sup>24</sup> as depicted in Fig. 4. After a transient solution, such as water, is deposited on the powder bed, it penetrates through the top layer under gravity and capillary pressure, where the nanoparticles are partially dissolved (particularly sharp edges), leading to soft nanoparticle surfaces, and small-size particles are transported into the pores between the large particles. As an appropriate hydrothermal process (pressure and temperature) is applied, the surface-softened nanoparticles deform, resulting in closer distances between the particles and full saturation or occupation of water in interparticle pores. Due to a higher chemical potential at the contact areas between the nanoparticles caused by capillary pressure, ionic species and/or atomic clusters diffuse through the water and precipitate on particle surfaces away from the stressed contact areas. As a result, the pores are fulfilled with precipitation that binds those particles together. The bonding between the particles can be further enhanced by completely evaporating the residual water in the pores, using an oven. Compared to other ceramic AM processes, the HTBJ process binds particles with an evaporative solution, which transiently evaporates as a green part is formed, and hence does not take up any space in the green parts, enabling an increased green density.

### Effect of Pressure on Green Density

The effects of pressure on green density are shown in Fig. 5a. Under the same temperature, the green density increased from 70% to over 85% with the increasing final pressure. This is because a higher pressure induces a higher capillary pressure in the powder, enabling a higher chemical potential to drive the mass transport towards the pores. The density reached an approximate plateau above a pressure of 450 MPa, which is determined by the

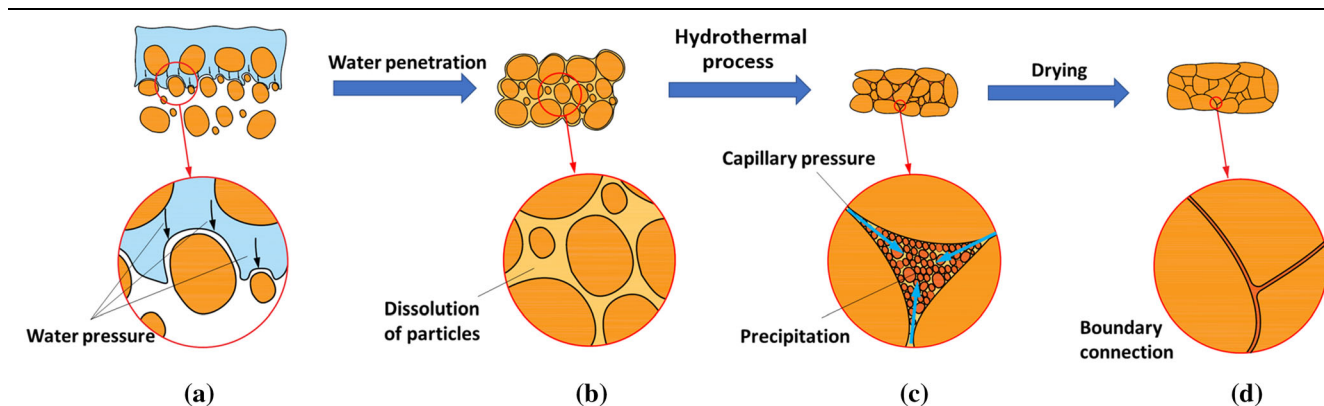


Fig. 4. Fusion mechanisms involved in HTBJ: (a) water deposition in the powder; (b) dissolution of nanoparticles in water; (c) precipitation of nanoparticles in a pore under a hydrothermal process; (d) solidification of the green part after drying.

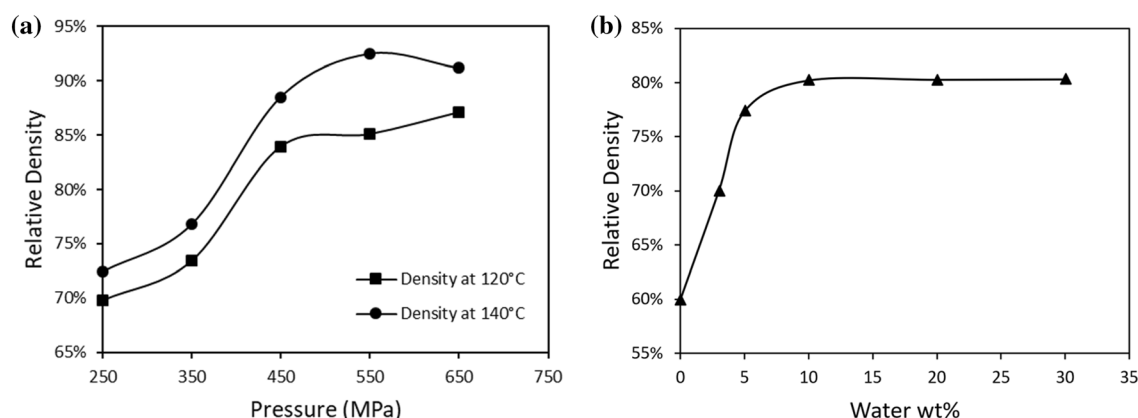


Fig. 5. Relative density of green parts achieved by HTBJ: (a) effects of final pressures and temperatures (water 10 wt.%); (b) effect of water concentration (350 MPa and 120°C).

degree of supersaturation of the ceramic material in water.

### Effect of Temperature on Green Density

Figure 5a shows that the green density increased by about 5% as the temperature increased from 120°C to 140°C. An explanation for this increase is that a higher temperature leads to a higher degree of solute supersaturation and a greater evaporation rate of water, which consequently contribute to more precipitates diffused into the pores. It should be noted that the density did not increase as the temperature continued to increase. Under a temperature of 180°C, for example, the powder was not successfully fused, and the powder compact was easily smashed in ultrasound. This may be because the evaporation rate of water exceeds the rate of atomic diffusion–precipitation, such that condensation of the dissolved phase stopped at sites close to the contact areas.

### Effect of Water Concentration on Green Density

Figure 5b shows that the green density increased dramatically from 60% to 80% as the water concentration increased from 0 wt.% to 10 wt.%. The density of the green part obtained without adding any water (i.e., 0%) was estimated as the packing density of the powder, since the achieved green part was too fragile to measure. Similar to the results shown in Fig. 5a, the green density reached a plateau above a water concentration of 10 wt.%. That is because the water concentration required for obtaining sufficient precipitates to occupy interparticle pores is related to the porosity of the powder compact under the given pressure and temperature conditions. When the water concentration is greater than the porosity, all the excess water will be expelled out of the powder compact as the pressure is applied, leaving a fixed concentration of water in the interparticle pores that results in the same green density.

### Microstructures of Fused Ceramics

The microstructures of the as-received powder and a green part fabricated with 10 wt.% water, 650 MPa and 120°C are shown in Fig. 6. The SEM images show that a dense green body can be achieved via the HTBJ process with a small porosity and sufficient strength. However, it remains unclear how the mass is transported during the HTBJ process, and how different process parameters influence the microstructures of the green body, which need further study in the future.

### Processing Map for Selective Fusion

The processing map constructed for the water concentration of 10 wt.% is given in Fig. 7. The red region depicts different combinations of temperature and final pressure that produced sufficiently strong green parts. It indicates that a green part can be obtained at a pressure as low as 12.5 MPa or a temperature as low as 80°C. The gray region denotes the process parameters that produce fragile green parts. The corresponding temperature and final pressure cannot effectively fuse the ceramic nanoparticles, which were easily smashed in the ultrasound. The blue region represents the temperatures and pressures that initialized the fusion of some nanoparticles but did not achieve sufficient strength.

### Test Cases

Several test cases were fabricated using an aqueous carbon ink as the transient solution, due to the excellent ink-jet printability in comparison to pure DI water. For transient solution deposition, the layer thickness was set as 500  $\mu\text{m}$ , and a pre-press pressure of 25 MPa and a print pass of 15 were used for each layer. For hydrothermal pressing, the final pressure and temperature were set as 350 MPa and 120°C, respectively, and the holding time was 20 min. Figure 8 shows a cross shape and “UI” characters. The fabrication accuracy was influenced

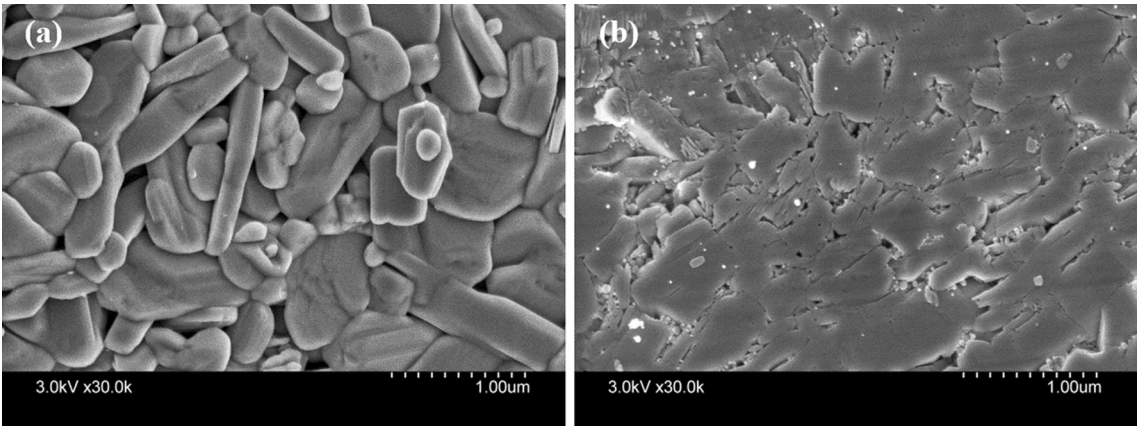


Fig. 6. Microstructures of (a) as-received V<sub>2</sub>O<sub>5</sub> powder, and (b) green part achieved by the HTBJ process (10 wt% water, 650 MPa and 120°C).

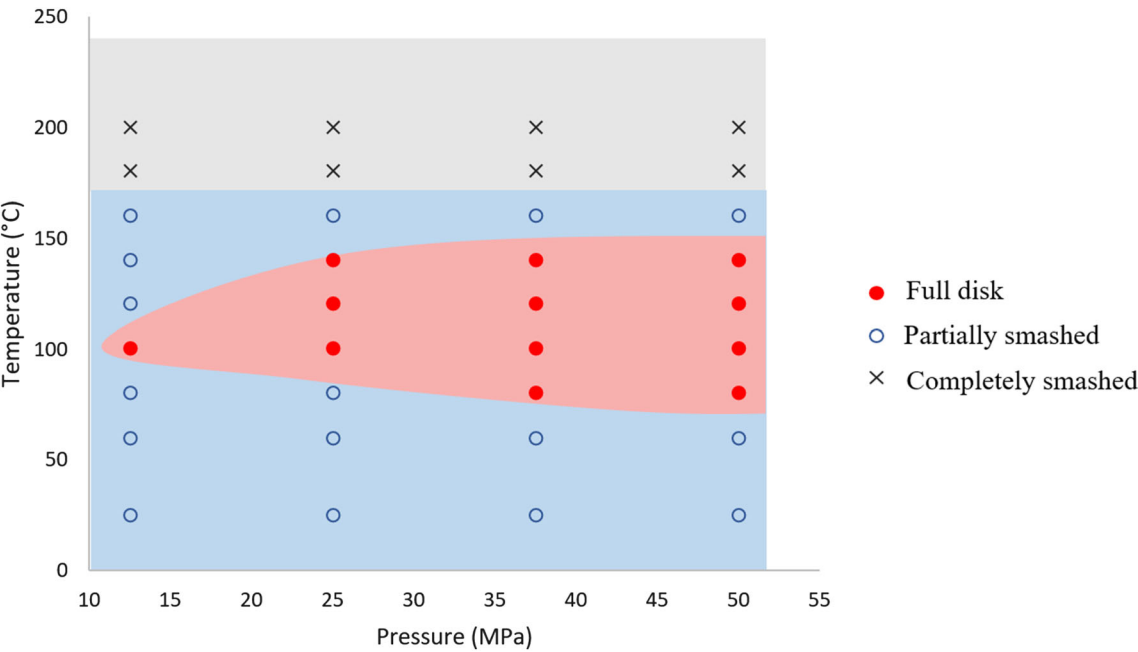


Fig. 7. Processing map for the water concentration of 10 wt%.



CAD	Results by HPBF	Density (g cm <sup>-3</sup> )
+		2.83 (84%)
UI		2.64 (79%)

Fig. 8. Test cases fabricated by the HTBJ process.

by the ink diffusion across the designed boundaries, which can be reduced by optimizing the layer thickness, and the pre-press and final press of the HTBJ process. The green densities of the achieved samples reached 84%, which is much higher than those reported in the literature, such as 60% by extrusion-based ceramic AM,<sup>25</sup> 67% by a slurry-based BJ process,<sup>10</sup> etc. It should be noted that the Glycol in the aqueous ink solution may play a partial role as a binder in bonding the particles. Further research is needed to quantify the effects of the water-modulated hydrothermal material interaction on the powder fusion and the final green density.

## CONCLUSION AND FUTURE WORK

In this paper, a new ceramic AM process, i.e., hydrothermal-assisted transient binder jetting (HTBJ), was developed to achieve green parts with high density. In the HTBJ process, a dense green part is fabricated through three major steps: transient solution deposition, hydrothermal pressing, and ultrasound elimination. In comparison to conventional ceramic AM processes, the HTBJ process eliminates the use of organic binders for shaping green parts, which significantly increases the density of green parts and enables the fabrication of functional ceramics with high performance, such as piezoelectric ceramics and transparent ceramics. The effects of process parameters (final pressing pressure, temperature, water concentration) on the achieved green density were investigated. A green density exceeding 90% was achieved when the final pressure and temperature were set as 550 MPa and 140°C, respectively. A processing map was constructed for the water concentration of 10 wt.%. Test cases highlight the feasibility of the HTBJ process in achieving complex ceramic structures with high density. Our future work will focus on optimizing the print pass, layer thickness, and pre-press and final press to further improve the fabrication quality of the HTBJ process.

## ACKNOWLEDGEMENTS

This research was funded by the Iowa Technology Institute at the University of Iowa.

## REFERENCES

1. L. He and X. Song, *JOM* 70, 407 (2018).
2. L. He, F. Fei, W. Wang and X. Song, *ACS Appl. Mater. Interfaces* 11, 18849 (2019).
3. M.L. Griffith and J.W. Halloran, *J. Am. Ceram. Soc.* 79, 2601 (1996).
4. D.L. Bourell, H.L. Marcus, J.W. Barlow, and J.J. Beaman, *Int. J. Powder Metall. (Princeton, N. J.)* 28, 369 (1992).
5. J.-P. Kruth, P. Mercelis, J. Van Vaerenbergh, L. Froyen, and M. Rombouts, *Rapid Prototype J.* 11, 26 (2005).
6. S.L. Sing, W.Y. Yeong, F.E. Wiria, B.Y. Tay, Z. Zhao, L. Zhao, Z. Tian, and S. Yang, *Rapid Prototype J.* 23, 611 (2017).
7. J. Moon, J.E. Grau, V. Knezevic, M.J. Cima, and E.M. Sachs, *J. Am. Ceram. Soc.* 85, 755 (2002).
8. G. Manogharan, M. Kioko, and C. Linkous, *JOM* 67, 660 (2015).
9. J. Gonzalez, J. Mireles, Y. Lin, and R.B. Wicker, *Ceram. Int.* 42, 10559 (2016).
10. J. Grau, J. Moon, S. Uhland, M. Cima and E. Sachs, *Solid Freeform Fabr. Symp. Proc.* 8, 371 (1997).
11. L.N. Rabinskiy, S.A. Sitnikov, V.A. Pogodin, A.A. Ripetskiy and Y.O. Solyaev, *Solid State Phenom.* 269, 37 (2017).
12. A.Y. Kumar, Y. Bai, A. Eklund, and C.B. Williams, *Addit. Manuf.* 24, 115 (2018).
13. M. Matsubara, T. Yamaguchi, K. Kikuta, and S.-I. Hirano, *Jpn. J. Appl. Phys.* 44, 258 (2005).
14. W. Li and J. Sun, *Med. Sci. Monit. Int. Med. J. Exp. Clin. Res.* 24, 3068 (2018).
15. U. Vogt, M. Gorbar, P. Dimopoulos-Eggenschwiler, A. Broenstrup, G. Wagner, and P. Colombo, *J. Eur. Ceram. Soc.* 30, 3005 (2010).
16. Y. Shi, W. Chen, L. Dong, H. Li, and Y. Fu, *Ceram. Int.* 44, 57 (2018).
17. H. Atkinson and S. Davies, *Metall. Mater. Trans. A* 31, 2981 (2000).
18. X. Huang, X. Zhang, Z. Hu, Y. Feng, J. Wei, X. Liu, X. Li, H. Chen, L. Wu, and H. Pan, *Opt. Mater.* 92, 359 (2019).
19. H. Zhang, H. Wang, H. Gu, X. Zong, B. Tu, P. Xu, B. Wang, W. Wang, S. Liu, and Z. Fu, *J. Eur. Ceram. Soc.* 38, 4057 (2018).
20. P. Kunchala and K. Kappagantula, *Mater. Des.* 155, 443 (2018).
21. H. Zhao, C. Ye, Z. Fan and Y. Shi, *Inter. Conf. Sen. Meas. Intel. Mater.* 4, 654 (2016).
22. H. Assaedi, F. Shaikh, and I.M. Low, *J. Asia. Ceram. Soc.* 4, 19 (2016).
23. H. Wu, Y. Cheng, W. Liu, R. He, M. Zhou, S. Wu, X. Song, and Y. Chen, *Ceram. Int.* 42, 17290 (2016).
24. J. Guo, H. Guo, A.L. Baker, M.T. Lanagan, E.R. Kupp, G.L. Messing, and C.A. Randall, *Angew. Chem.* 55, 11457 (2016).
25. A. Zocca, P. Colombo, C.M. Gomes, and J. Günster, *J. Am. Ceram. Soc.* 98, 1983 (2015).

**Publisher's Note** Springer Nature remains neutral with regard to jurisdictional claims in published maps and institutional affiliations.